# Backreaction of scalar waves on black holes at low frequencies

Marco de Cesare[1,2,*] and Roberto Oliveri[3,†]

[1]*Dipartimento di Fisica "Ettore Pancini", Università di Napoli Federico II, Napoli 80125, Italy*
[2]*INFN, Sezione di Napoli, Napoli 80125, Italy*
[3]*LUTH, Laboratoire Univers et Théories, Observatoire de Paris, CNRS, Université PSL, Université Paris Cité, 5 place Jules Janssen, 92190 Meudon, France*

(Received 22 May 2023; accepted 28 July 2023; published 23 August 2023)

We study the accretion of a Schwarzschild black hole due to spherically symmetric perturbations sourced by a minimally coupled massless scalar field. The backreaction of the black hole to low-frequency ingoing scalar waves is computed analytically as a second-order perturbative effect, using matched asymptotic expansions to relate the behavior of the scalar field in the vicinity of the horizon and at null infinity. As an application of our results, we compute the mass increase due to (i) ingoing wave packets with an arbitrary profile and (ii) incoherent radiation. Our results could serve as a model for the backreaction of environmental scalar fields on black holes.

DOI: 10.1103/PhysRevD.108.044050

## I. INTRODUCTION

Astrophysical black holes do not exist in a vacuum. They form as a result of the gravitational collapse of matter, and their accretion dynamics after formation is determined by the nonlinear interaction of gravity with matter fields. The mass of a black hole grows in time due to the flux of matter energy-momentum and gravitational waves through the black-hole horizon. In dynamical situations, different quasi-local definitions have been proposed for the black-hole horizon, among which the best known are the *future outer trapping horizon* [1], the *dynamical horizon* [2], or the *slowly evolving horizon* [3] (see also Refs. [4–6]). These definitions replace the standard notion of the *event horizon*, which is teleological in nature and thus cannot be probed by any physical means.

The laws that determine the evolution of the black-hole horizon are quasi-local. However, in many practical situations, one may want to recover a global picture of the spacetime and thus relate the evolution of a black hole to the asymptotic behavior of matter fields far from the black hole. In particular, in the case of scattering from a black hole, it is of interest to compute the resulting mass increase due to the partial absorption of waves with a given profile. While the backreaction due to steady-state accretion of matter onto a black hole has been studied in Ref. [7] (see also Refs. [8,9]), in more general dynamical situations, the problem remains unexplored.

In this work, we study analytically the evolution of the black-hole mass in response to low-frequency massless scalar field perturbations originating from past null infinity in spherical symmetry. Due to the presence of the black hole, the scalar field feels an effective potential barrier. As a consequence, ingoing waves get scattered off the barrier and thus are partly absorbed by the black hole and partly reflected toward future null infinity [10]. The low frequency of the perturbations ensures that the quasi-normal modes of the system are not excited during the scattering process; hence, the reflected signal is almost undistorted. The flux of energy through the black-hole horizon results in a mass increase of the black hole itself or, equivalently, in the expansion of the future outer trapping horizon.

We adopt a perturbative approach to analyze the dynamics of the system, assuming a Schwarzschild geometry for the background and spherically symmetric perturbations for both matter and the geometry. The assumption of spherical symmetry is not too restrictive, since the low-frequency scattering cross section for a scalar field is dominated by the monopole contribution [10]. First, we solve the dynamics of the scalar field in Fourier space and in the low-frequency regime, deriving approximate analytical solutions that are valid in the regions far from the black hole and close to its Schwarzschild radius. The two asymptotics are then suitably matched in their overlap region to compute the transmission and reflection coefficients, following the approach in Ref. [11]. After transforming back to position space to build wave packets, we find a novel relation between the transmitted and ingoing wave packets. Next, the backreaction of the scalar wave on the black-hole mass is obtained as a second-order effect in perturbation theory. We derive for the first time a simple closed-form expression for the accretion rate in terms of the ingoing wave packet that can have arbitrary profile.

*marco.decesare@na.infn.it
†roberto.oliveri@obspm.fr

 

The mass increase in turn leads to a decrease of the surface gravity, whose evolution is also obtained analytically. Our results shed light on the evolution of the trapping horizon due to the scattering of massless fields and provide us with an analytical handle that could serve as a complement to numerical relativity simulations.

We then apply our results to the special cases of coherent and incoherent radiation, computing the relative mass increase as a function of the ingoing null coordinate. In the coherent case, the mass has two plateaux: one in the past corresponding to the background value of the mass and one in the future corresponding to the final value of the black-hole mass after the wave packet has scattered. Moreover, we observe two general features: (i) the mass increase displays horizontal inflection points in correspondence with the inflection points of the ingoing wave packet, and (ii) for fixed ingoing flux, the magnitude of the mass increase is greater for more sharply peaked wave packets. This is in agreement with features observed in numerical simulations [12]. In the case of incoherent radiation, we find that the accretion rate is proportional to the ingoing flux, with a proportionality constant that is fully determined by the amplitude in Fourier space and by the black-hole mass.

## II. SCALAR PERTURBATIONS ON SCHWARZSCHILD

Throughout this work, we focus on spherically symmetric configurations for both matter and the geometry. The most general spherically symmetric metric in four spacetime dimensions reads

$$\mathrm{d}s^2 = -A(t,r)e^{\nu(t,r)}\mathrm{d}t^2 + A^{-1}(t,r)\mathrm{d}r^2 + r^2\mathrm{d}\Omega^2, \quad (2.1)$$

with $A(t,r) = 1–2m(t,r)/r$, where $m(t,r)$ is the Misner-Sharp mass (i.e., the energy contained in a spherical shell with areal radius $r$). We assume a Schwarzschild background with constant mass $M$.

We introduce matter perturbations in the form of a minimally coupled scalar field $\phi$, with energy-momentum tensor[1] $T_{ab} = \partial_a\phi\partial_b\phi - \frac{1}{2}g_{ab}(g^{cd}\partial_c\phi\partial_d\phi)$. The background value of the scalar field $\phi$ is zero; hence, we treat $\phi$ as a first-order quantity in the perturbative expansion. Moreover, since $T_{ab}$ is quadratic in $\phi$, the presence of the scalar field only affects the geometry starting from second order in perturbation theory. The metric (2.1) is then expanded perturbatively around the Schwarzschild background, with the ansätze $m(t,r) = M + m^{(1)}(t,r) + m^{(2)}(t,r) + \cdots$ and $\nu(t,r) = \nu^{(1)}(t,r) + \nu^{(2)}(t,r) + \cdots$.

Expanding the Einstein field equations $G^a{}_b = 8\pi T^a{}_b$, we find to first order in perturbation theory $\mathrm{d}m^{(1)} = \mathrm{d}\nu^{(1)} = 0$. This implies that the first-order corrections $m^{(1)}$ and $\nu^{(1)}$ are constant and therefore merely amount to a redefinition of the background mass and time gauge; hence, we can set them to zero without loss of generality. Furthermore, the scalar field obeys the wave equation $\Box\phi = 0$. The dynamics of $\phi$ will be analyzed in detail in Sec. III.

To second order in the perturbative expansion, the $(t,t)$ and $(t,r)$ components of the field equations read

$$\frac{\partial m^{(2)}}{\partial r} = 2\pi r^2\left[\left(1-\frac{2M}{r}\right)^{-1}\left(\frac{\partial\phi}{\partial t}\right)^2 + \left(1-\frac{2M}{r}\right)\left(\frac{\partial\phi}{\partial r}\right)^2\right], \quad (2.2a)$$

$$\frac{\partial m^{(2)}}{\partial t} = 4\pi r^2\left(1-\frac{2M}{r}\right)\frac{\partial\phi}{\partial t}\frac{\partial\phi}{\partial r}. \quad (2.2b)$$

From the $(r,r)$ component of the field equations, one finds the equation for $\nu^{(2)}$; however, for our purposes, we will only be concerned with $m^{(2)}$.

Introducing the Regge-Wheeler tortoise coordinate $r_* = r + 2M\log|r/(2M) - 1|$ and taking the near-horizon limit $r_* \to -\infty$ of Eqs. (2.2a) and (2.2b), we obtain

$$\frac{\partial m^{(2)}}{\partial r_*} \approx 2\pi\left[\left(\frac{\partial(r\phi)}{\partial t}\right)^2 + \left(\frac{\partial(r\phi)}{\partial r_*}\right)^2\right], \quad (2.3a)$$

$$\frac{\partial m^{(2)}}{\partial t} \approx 4\pi\frac{\partial(r\phi)}{\partial t}\frac{\partial(r\phi)}{\partial r_*}. \quad (2.3b)$$

Finally, introducing the null coordinates $u = t - r_*$, $v = t + r_*$ and combining Eq. (2.3), we obtain

$$\frac{\partial m^{(2)}}{\partial v} \approx 4\pi\left(\frac{\partial(r\phi)}{\partial v}\right)^2, \qquad \frac{\partial m^{(2)}}{\partial u} \approx -4\pi\left(\frac{\partial(r\phi)}{\partial u}\right)^2. \quad (2.4)$$

Equation (2.4) will be used in Sec. IV to determine the corrections to the black-hole mass.

## III. SCALAR FIELD DYNAMICS: SCATTERING OF WAVE PACKETS

The scalar field $\phi$ obeys the wave equation $\Box\phi = 0$, which in Schwarzschild coordinates, reads

$$\frac{\partial^2\phi}{\partial t^2} - \frac{\Delta}{r^4}\frac{\partial}{\partial r}\left(\Delta\frac{\partial\phi}{\partial r}\right) = 0, \quad (3.1)$$

with $\Delta \equiv r^2 - 2Mr$. Taking the Fourier transform $\phi(t,r) = (2\pi)^{-1}\int\mathrm{d}\omega R(\omega,r)e^{-i\omega t}$ and introducing a new radial coordinate $x \equiv r/(2M) - 1$, we bring Eq. (3.1) to the form [11]

[1] It has been proved in Ref. [13] that in the presence of a massless scalar field acting as null dust, the metric cannot have the Vaidya form.

$$x^2(1+x)^2\frac{\mathrm{d}^2R}{\mathrm{d}x^2}+x(1+x)(1+2x)\frac{\mathrm{d}R}{\mathrm{d}x}+(2M\omega)^2(1+x)^4R=0. \tag{3.2}$$

We focus on modes that are purely ingoing at the horizon, i.e., $R\sim\mathcal{T}(\omega)e^{-i\omega r_*}/r$ as $r_*\to-\infty$, where $\mathcal{T}(\omega)$ is the transmission coefficient. Far from the black hole, we require that the solution be a linear superposition of ingoing and outgoing waves, $R\sim\mathcal{I}(\omega)e^{-i\omega r_*}/r+\mathcal{R}(\omega)e^{i\omega r_*}/r$ as $r_*\to\infty$, where $\mathcal{I}(\omega)$ and $\mathcal{R}(\omega)$ are the incidence and reflection coefficients. In terms of the $x$ coordinate, these boundary conditions read as $R\sim\mathcal{T}(\omega)x^{-i(2M\omega)}/(2M)$ as $x\to0$, and $R\sim\mathcal{I}(\omega)e^{-i(2M\omega)x}/(2Mx)+\mathcal{R}(\omega)e^{i(2M\omega)x}/(2Mx)$ as $x\to+\infty$. In the following, we will often omit the $\omega$ dependence to make the notation lighter.

We are interested in solving Eq. (3.2) in the low-frequency limit, so as not to excite the quasi-normal modes. To this end, we introduce a small dimensionless parameter $\epsilon\equiv2M\omega$ such that $|\epsilon|\ll1$. Approximate analytical solutions for Eq. (3.2) can then be found in the near region, close to the Schwarzschild radius of the background geometry and in the far region at large distances from the black hole. Next, by matching the two asymptotics, we can determine the relations between the transmission, reflection, and incidence coefficients, thus obtaining a global approximation to the solution of Eq. (3.2). In the derivation of the asymptotics, we follow similar steps as in Ref. [11,14]. However, there are important subtleties in the case of monopole perturbations here considered that have not been discussed in these references.

### A. Solution in the near region

Here, we focus on the regime $x|\epsilon|\ll1$, where Eq. (3.2) can be approximated as

$$x^2(1+x)^2\frac{\mathrm{d}^2R}{\mathrm{d}x^2}+x(1+x)(1+2x)\frac{\mathrm{d}R}{\mathrm{d}x}+\epsilon^2(1+4x)R=0. \tag{3.3}$$

Note that we included a term $\sim\epsilon^2x$ in the prefactor of $R$ that arises from the linearization of $(1+x)^4$, which has been overlooked in previous works; see, e.g., Refs. [11,14,15] for $l=0$. Equation (3.3) can be solved exactly. With our choice of boundary conditions, the solution reads

$$R_{\mathrm{near}}(x)=ax^{-i\epsilon}(1+x)^{\sqrt{3}\epsilon}\times{}_2F_1(1+(\sqrt{3}-i)\epsilon,(\sqrt{3}-i)\epsilon;1-2i\epsilon;-x), \tag{3.4}$$

where $a$ is an integration constant, and ${}_2F_1$ is the hypergeometric function. For small values of $x$

$$R_{\mathrm{near}}(x)\approx ax^{-i\epsilon},\quad x\to0, \tag{3.5}$$

and thus we identify the transmission coefficient to be $\mathcal{T}=2Ma$. In the large-$x$ limit, $R_{\mathrm{near}}$ should be matched to the far-region solution. For this reason, we compute the leading-order asymptotics of the solution (3.4) in the limit where $x\gg1$, retaining terms up to first order in $\epsilon$, which gives[2]

$$R_{\mathrm{near}}(x)\approx\frac{\mathcal{T}}{2M}\left(1+\frac{i\epsilon}{x}\right),\quad x\to+\infty. \tag{3.6}$$

### B. Solution in the far region

At large distances from the hole, $x\gg1$, we can approximate Eq. (3.2) as

$$\frac{\mathrm{d}^2R}{\mathrm{d}x^2}+\frac{2}{x}\frac{\mathrm{d}R}{\mathrm{d}x}+\epsilon^2\left(1+\frac{2}{x}\right)R=0. \tag{3.7}$$

The general solution of Eq. (3.7) is a linear combination of the confluent hypergeometric function $U$ and the Kummer confluent hypergeometric function ${}_1F_1$

$$R_{\mathrm{far}}(x)=e^{-i|\epsilon|x}(c_1U(1+i|\epsilon|,2,2i|\epsilon|x)+c_2{}_1F_1(1+i|\epsilon|;2;2i|\epsilon|x)), \tag{3.8}$$

with $c_1$, $c_2$ integration constants. Taking the large-$x$ limit of the solution (3.8), we obtain

$$R_{\mathrm{far}}(x)\approx\frac{1}{2i|\epsilon|x}((c_1-c_2)e^{-i|\epsilon|x}+c_2e^{i|\epsilon|x}),\qquad x\to+\infty. \tag{3.9}$$

Recalling the definition of the incidence and reflection coefficients, we find from Eq. (3.9) that $\mathcal{I}=(c_1-c_2)/(2i\omega)$, $\mathcal{R}=c_2/(2i\omega)$ for $\omega>0$, whereas $\mathcal{I}=c_2/(2i|\omega|)$, $\mathcal{R}=(c_1-c_2)/(2i|\omega|)$ for $\omega<0$.

[2]We note that the large-$x$ asymptotics of the hypergeometric function (used, for instance, in Refs. [11,14], where nonzero values are assumed for the black-hole spin and the angular momentum of the scalar field)

$${}_2F_1(a,b;c;-x)\approx\frac{\Gamma(b-a)\Gamma(c)}{\Gamma(b)\Gamma(c-a)}x^{-a}+\frac{\Gamma(a-b)\Gamma(c)}{\Gamma(a)\Gamma(c-b)}x^{-b}$$

does not apply in our case, since $a-b$ is an integer; see Ref. [16]. In this case, extra care is needed. To obtain the asymptotics (3.6), we use the integral representation ${}_2F_1(a,b;c;-x)=\frac{\Gamma(c)}{\Gamma(b)\Gamma(c-b)}\int_0^\infty\mathrm{d}t\,t^{-b+c-1}(t+1)^{a-c}(t-x+1)^{-a}$, with $\Re(c)>\Re(b)>0$ and expand the integrand in the limit of large $x$; then, we substitute the asymptotics thus obtained in (3.4) and expand the result to first order in $\epsilon$.

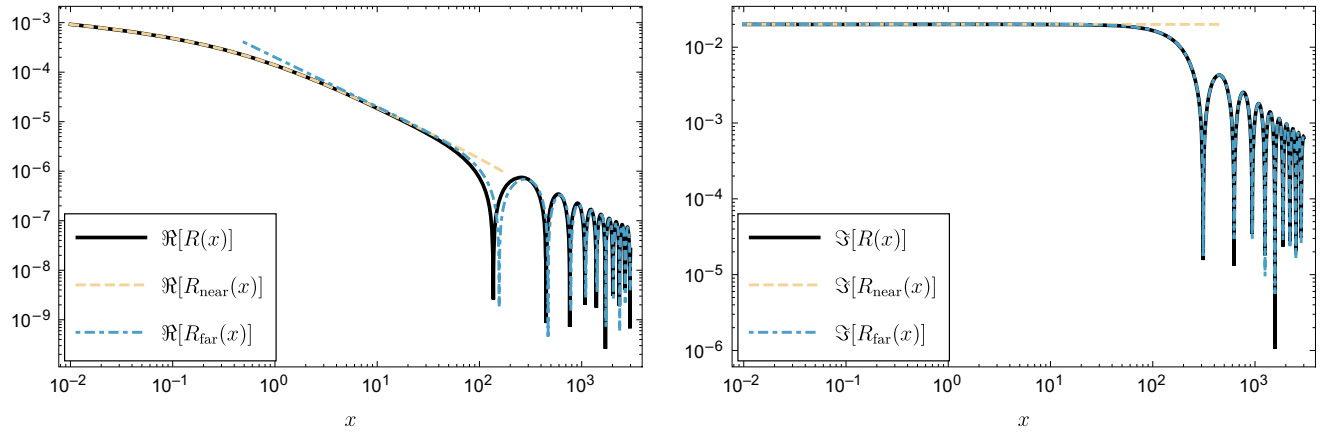


FIG. 1. The plots show the real (left panel) and imaginary (right panel) parts of the numerical solution of Eq. (3.2) satisfying ingoing boundary conditions at the horizon, along with the corresponding asymptotics (3.4) and (3.8) in the near and far regions, for $\epsilon = 10^{-2}$ and $\mathcal{I} = 1$, in units such that $2M = 1$. The two asymptotics are matched in their overlap region using Eq. (3.11).

In the limit $x|\epsilon| \ll 1$, we have

$$R_{\rm far}(x) \approx \frac{1}{2M}\left(i\epsilon(\mathcal{R}-\mathcal{I}) + \frac{(\mathcal{R}+\mathcal{I})(1+i\gamma|\epsilon|)}{x}\right), \quad x|\epsilon| \to 0, \tag{3.10}$$

where $\gamma$ is the Euler-Mascheroni's constant.

### C. Matched asymptotics

We can match the large-$x$ asymptotics of the near-region solution (3.6) with the small-$x$ asymptotics of the far-region solution (3.10), obtaining for the reflection and transmission coefficients[3]

$$\begin{aligned}\mathcal{T} &= -2i\epsilon\mathcal{I} + \mathcal{O}(\epsilon^3)\\ \mathcal{R} &= (-1+2\epsilon^2)\mathcal{I} + \mathcal{O}(\epsilon^3).\end{aligned} \tag{3.11}$$

Thus, the relation $|\mathcal{T}|^2 + |\mathcal{R}|^2 = |\mathcal{I}|^2$ is satisfied up to $\mathcal{O}(\epsilon^3)$ terms. In Fig. 1, we display the asymptotics corresponding to the near and far regions, matched using Eq. (3.11), alongside the numerical solution of Eq. (3.2).

### D. Scattering of wave packets

Assuming an incident wave packet $\phi_{\rm in}(v,r) = (2\pi r)^{-1}\int d\omega \mathcal{I}(\omega)e^{-i\omega v}$, the reflected and transmitted wave packets are, respectively, given by $\phi_{\rm out}(u,r) = (2\pi r)^{-1}\times \int d\omega \mathcal{R}(\omega)e^{-i\omega u}$, $\phi_{\rm H,in}(v,r) = (2\pi r)^{-1}\int d\omega \mathcal{T}(\omega)e^{-i\omega v}$ (where $u \equiv t - r_*$, $v \equiv t + r_*$ are null coordinates). Reality of $\phi_{\rm in}$ implies the condition $\bar{\mathcal{I}}(\omega) = \mathcal{I}(-\omega)$; furthermore, Eq. (3.11) ensures that similar conditions are also obeyed by $\mathcal{T}$ and $\mathcal{R}$. From the above, under the assumption that $\mathcal{I}(\omega)$ has support on low frequencies, we obtain for the transmitted wave packet

$$\begin{aligned}\phi_{\rm H,in}(v,r) &= \frac{1}{2\pi r}\int_{-\infty}^{+\infty} d\omega(-2i)(2M\omega)\mathcal{I}(\omega)e^{-i\omega v}\\ &= \frac{4M}{r}\frac{\rm d}{{\rm d}v}(r\phi_{\rm in}(v,r)),\end{aligned} \tag{3.12}$$

while the reflected packet reads[4]

$$\begin{aligned}\phi_{\rm out}(u,r) &= \frac{1}{2\pi r}\int_{-\infty}^{+\infty} d\omega(-1+2(2M\omega)^2)\mathcal{I}(\omega)e^{-i\omega u}\\ &= -\phi_{\rm in}(u,r) - \frac{8M^2}{r}\frac{{\rm d}^2}{{\rm d}u^2}(r\phi_{\rm in}(u,r)).\end{aligned} \tag{3.13}$$

The ingoing and outgoing energy fluxes are, respectively,

$$\begin{aligned}\mathcal{F}_{\rm in}(v) &= 4\pi r^2\left(\frac{\partial}{\partial v}\phi_{\rm in}(v,r)\right)^2,\\ \mathcal{F}_{\rm out}(u) &= 4\pi r^2\left(\frac{\partial}{\partial u}\phi_{\rm out}(u,r)\right)^2.\end{aligned} \tag{3.14}$$

The fraction of energy absorbed by the hole is

$$Z = 1 - \frac{\int_{-\infty}^{+\infty} du\mathcal{F}_{\rm out}(u)}{\int_{-\infty}^{+\infty} dv\mathcal{F}_{\rm in}(v)}. \tag{3.15}$$

## IV. BACKREACTION EFFECTS ON THE BLACK-HOLE MASS

The backreaction effects of matter on the black-hole mass are determined by Eq. (2.4). We note that in the general case,

[3]The error terms in Eq. (3.11) have been estimated by including higher-order terms in the near- and far-region asymptotics.

[4]The total derivatives in the last steps of Eqs. (3.12) and (3.13) are due to the fact that the quantity $r\phi_{\rm in}(v,r)$ has no dependence on $r$.

the scalar field may include both an ingoing and an outgoing component in the near-horizon region. Assuming ingoing boundary conditions as in Sec. III, Eq. (2.4) gives $m^{(2)} \approx m^{(2)}(v)$ in the $u \to +\infty$ limit where the horizon of the background is approached. This implies that the mass of the perturbed black hole is $\bar{M}(v) = M + \Delta M(v)$, where $\Delta M(v) \equiv \lim_{u\to+\infty} m^{(2)}(u, v)$. Therefore, combining Eqs. (2.4) and (3.12), we obtain our main result

$$\frac{\mathrm{d}(\Delta M)}{\mathrm{d}v} \approx 64\pi M^2 \left(\frac{\mathrm{d}^2(r\phi_{\mathrm{in}})}{\mathrm{d}v^2}\right)^2. \tag{4.1}$$

Equation (4.1) also determines the black-hole trapping horizon as $r_H(v) = 2(M + \Delta M(v))$.[5] Integrating Eq. (4.1), we obtain the mass of the evolving black hole

$$\bar{M}(v) = M + 64\pi M^2 \int_{-\infty}^{v} \mathrm{d}v \left(\frac{\mathrm{d}^2(r\phi_{\mathrm{in}})}{\mathrm{d}v^2}\right)^2. \tag{4.2}$$

Combining Eqs. (4.2) and (3.15), we find the absorption coefficient $Z \approx (M_{\mathrm{final}} - M)/\mathcal{F}_{\mathrm{in}}^{\mathrm{TOT}}$, where $M_{\mathrm{final}} \equiv \lim_{v\to+\infty} \bar{M}(v)$ and $\mathcal{F}_{\mathrm{in}}^{\mathrm{TOT}} \equiv \int_{-\infty}^{\infty} \mathrm{d}v \mathcal{F}_{\mathrm{in}}(v)$ is the total ingoing energy flux. A Carter-Penrose diagram representing the evolution of a black hole in response to the scattering of a wave packet is shown in Fig. 2.

A geometric definition for the surface gravity of a dynamical black hole was given in Ref. [19], where it reads as $\kappa \equiv \frac{1}{2}(*d*dr)$,[6] which in spherical symmetry and in coordinates $(v, r)$ reduces to $\kappa(v) = (1 - 2\frac{\partial m(v,r)}{\partial r})/(4\bar{M}(v))$, where the rhs is evaluated at the horizon. Changing coordinates and using Eq. (2.3), we obtain $\frac{\partial m(v,r)}{\partial r} \propto (\frac{\partial(r\phi)}{\partial u})^2$ in the $r_* \to -\infty$ limit, which vanishes for purely ingoing boundary conditions at the horizon. Hence, we obtain

$$\kappa(v) = \frac{1}{4\bar{M}(v)}, \tag{4.3}$$

which is monotonically decreasing. For any given profile of the scalar field, including the cases considered in the next Sec. V, $\kappa(v)$ can be computed analytically.

## V. PHYSICAL APPLICATIONS

Equation (4.1) predicts that the black-hole mass is monotonically increasing in time, consistently with Hayward's *area increase theorem* [1], since the scalar field obeys the null energy condition. Moreover, Eq. (4.1) gives the exact accretion rate of the black-hole mass as a response to the infalling scalar field, given an arbitrary profile for the ingoing wave $\phi_{\mathrm{in}}$ (so long as its power spectrum is peaked on low frequencies). It applies for coherent as well as incoherent radiation, which we analyze in the following.

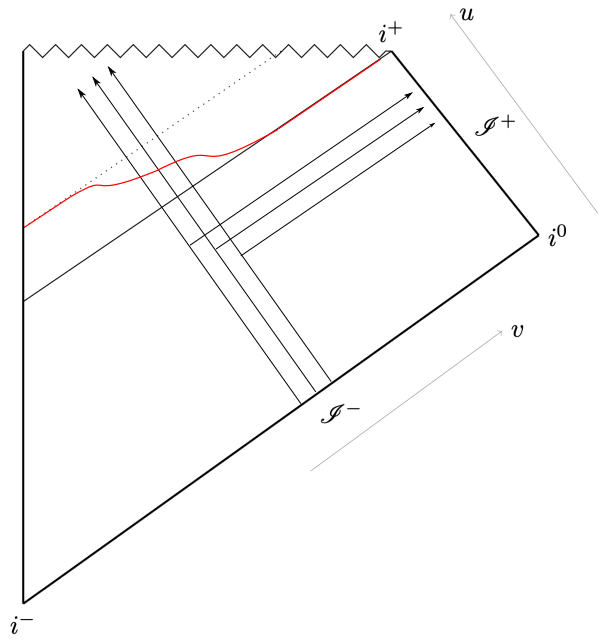


FIG. 2. Carter-Penrose diagram depicting the scattering of a wave packet by a spherically symmetric black hole and the consequent backreaction on the geometry. The *future outer trapping horizon* (red curve) is spacelike and interpolates between the event horizon of the Schwarzschild background (dotted line) and the event horizon of the perturbed spacetime (thick line).

### A. Coherent radiation

As an example, we compute the relative mass increase due to infalling wave packets with different profiles, as shown in Fig. 3. As a general feature, for a fixed ingoing flux, the final mass is higher for wave packets that are more sharply peaked. Moreover, inflection points of the wave packets correspond to the horizontal inflection points of the evolving black-hole mass. In turn, these correspond to inflection points of the monotonically decreasing surface gravity.

### B. Incoherent radiation

We consider ingoing radiation with $\mathcal{I}(\omega) = A(\omega)e^{-i\varphi_\omega}$, with a random phase $\varphi_\omega$. This is in part similar to the *random phase model* for wave dark matter [20], although in our case, the scalar field is massless (whereas wave dark matter must be nonrelativistic). The amplitude $A(\omega)$ is real and needs not be stochastic. The two-point function is

[5]More precisely, this is a future outer trapping horizon according to Hayward's definition [1], since $\theta_l = 0$, $\theta_n < 0$, and $\pounds_n \theta_l < 0$ (where $l^a$ and $n^a$ are future pointing radial null vectors, respectively, outward and inward directed). In the case at hand, the last condition follows from the fact that the scalar field obeys the null energy condition; see also Refs. [17,18].

[6]With $*$ and $d$ we denote, respectively, the Hodge dual and the exterior derivative in the $(t, r)$ space normal to the two-sphere.

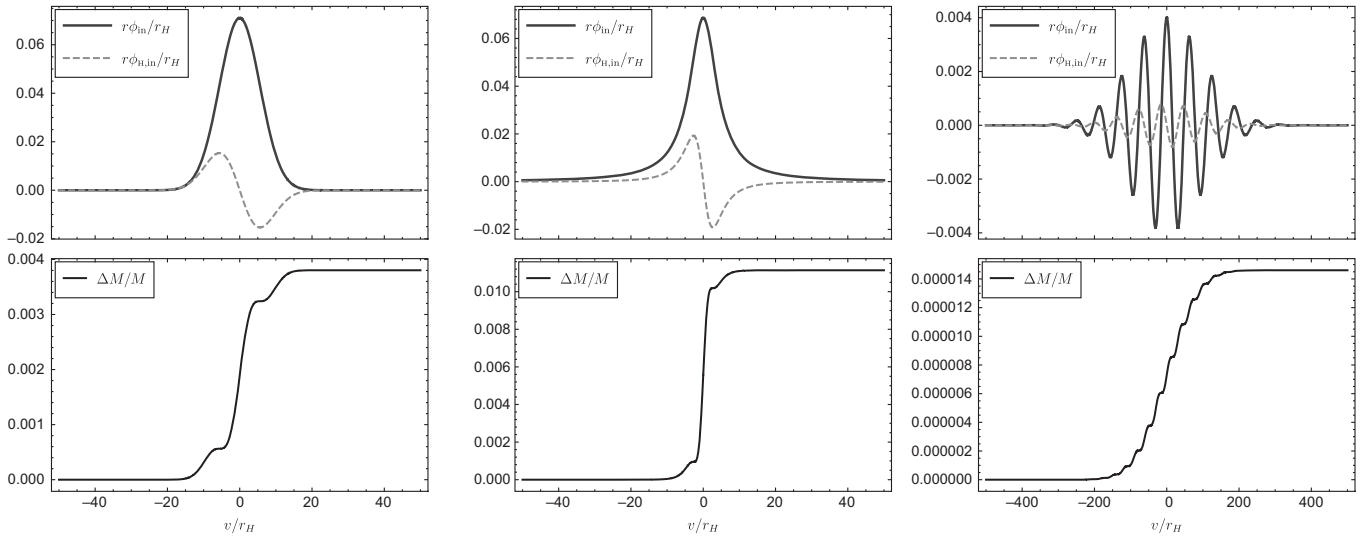


FIG. 3. We show the evolution of the black-hole mass corresponding to different profiles for the ingoing pulse. The leftmost and central figures correspond to a Gaussian and Lorentzian wave packets, respectively, with the same normalization and total energy flux. More specifically, these are given by $\phi_{\rm in}(v,r)=\frac{A}{\sqrt{2\pi}\sigma r}\exp\left(-\frac{(v-v_0)^2}{2\sigma^2}\right)$ and $\phi_{\rm in}(v,r)=\frac{A}{\pi r}\frac{\gamma}{\gamma^2+(v-v_0)^2}$, with $A=r_H^2$, $\mathcal{F}_{\rm in}^{\rm TOT}=10^{-2}r_H$ (the values of $\sigma$ and $\gamma$ are fixed accordingly: $\sigma\simeq 5.617r_H$, $\gamma\simeq 4.642r_H$), where $r_H$ is the background Schwarzschild radius. The origin of the horizontal axis has been shifted so that $v_0=0$. The rightmost plots correspond instead to a modulated Gaussian $\phi_{\rm in}(v,r)=\frac{A}{\sqrt{2\pi}\sigma r}\exp\left(-\frac{(v-v_0)^2}{2\sigma^2}\right)\cos\left(\omega(v-v_0)\right)$, with $A=r_H^2$, $\omega=10^{-1}/r_H$ and $\sigma=10^2 r_H$. We note the multiple horizontal inflection points corresponding to the inflection points of the ingoing pulse.

assumed to be $\langle e^{-i\varphi_\omega}e^{i\varphi_{\omega'}}\rangle=2\pi C\delta(\omega-\omega')$, where $C$ is a positive constant with dimensions of frequency. The expectation value of the ingoing flux is

$$\langle\mathcal{F}_{\rm in}(v)\rangle=2C\int_{-\infty}^{+\infty}{\rm d}\omega A(\omega)A(-\omega)\omega^2. \tag{5.1}$$

Note that $\langle\mathcal{F}_{\rm in}(v)\rangle$ does not depend on $v$ in this model. Then, taking the expectation value of Eq. (4.1), we obtain

$$\begin{aligned}\left\langle\frac{{\rm d}(\Delta M)}{{\rm d}v}\right\rangle&\approx 32CM^2\int_{-\infty}^{+\infty}{\rm d}\omega A(\omega)A(-\omega)\omega^4\\&\approx 16\left(\frac{\int_{-\infty}^{+\infty}{\rm d}\omega A(\omega)A(-\omega)\omega^4}{\int_{-\infty}^{+\infty}{\rm d}\omega A(\omega)A(-\omega)\omega^2}\right)M^2\langle\mathcal{F}_{\rm in}\rangle.\end{aligned} \tag{5.2}$$

Thus, the accretion rate is fully determined by the second and fourth moments of the product $A(\omega)A(-\omega)$. In particular, if we assume a Gaussian profile $A(\omega)=\mathcal{A}\exp(-(\omega-\bar{\omega})^2/(2\sigma^2))$, we obtain[7]

$$\left\langle\frac{{\rm d}(\Delta M)}{{\rm d}v}\right\rangle\approx 24\sigma^2M^2\langle\mathcal{F}_{\rm in}\rangle. \tag{5.3}$$

Once again, we observe that the accretion rate depends on the variance of the incoming wave packets, and it is greater for larger $\sigma$. The expectation value of the surface gravity $\langle\kappa(v)\rangle$ is monotonically decreasing with a constant rate in this model.

## VI. DISCUSSION

We investigated the low-frequency response of a Schwarzschild black hole to wave packets emitted in the far past. Our approach relies on second-order perturbation theory for the Einstein field equations with a minimally coupled massless scalar field obeying purely ingoing boundary conditions at the horizon. Our main results are presented in Sec. IV and shed light into the evolution of the trapping horizon as a result of the backreaction of low-frequency scalar waves. Equation (4.1) gives a closed-form formula for the accretion rate of the black hole that is controlled by the profile of the ingoing wave. The trapping horizon can be readily obtained from the evolution of the mass, Eq. (4.2). For wave packets, the trapping horizon interpolates between the event horizon of the Schwarzschild background and that of the perturbed spacetime, while for incoherent radiation, the horizon grows with a constant rate. Furthermore, our analytical results explain the qualitative features observed in numerical simulations of a black hole accreting wave packets of scalar radiation [12].

Our results could be relevant to model environmental effects in the evolution of black holes. In fact, scalar fields play an important role in cosmology, where they are responsible for the accelerated expansion of the universe at early times, and may play the role of dark matter at late

[7]Note that, within our low-frequency approximation, $A(\omega)$ must be peaked on low frequencies, i.e., $\bar{\omega}M\ll 1$ and $\sigma M\ll 1$.

times [20]. In future work, we will extend our analysis to nonasymptotically flat spacetimes and include scalar fields with a general potential to study the evolution of black holes in these scenarios. Moreover, our setup could be generalized further to massive complex scalar fields, which can support a black-hole hair [21] and may form clouds that are responsible for relativistic drag forces exerted on black holes [15,22]. Our analysis can be further generalized to also include hydrodynamic matter, which would allow for a comparison of our setup with recent studies on Bondi-Hoyle-Lyttleton accretion [23].

This work can be further extended in several directions. One can attempt to move beyond the low-frequency regime, either by matching the near and far-zone asymptotics obtained for a finite frequency $\omega$ or by including higher-order corrections in the expansion for small $\epsilon = 2M\omega$ and then solving the second-order perturbative equations to compute the backreaction on the mass. It would also be interesting to understand how the backreaction of massless fields is affected by a nonzero angular momentum of the black hole; while there are some numerical studies on this topic [24,25], analytically this question remains unexplored. Lastly, the cosmological analog of the classical backreaction problem considered in this paper will help us to shed light on the effects of cosmic expansion and more general matter fields on the evolution of primordial black holes. We will address these open questions in upcoming work.

## ACKNOWLEDGMENTS

We thank Eric Gourgoulhon and Carlos Herdeiro for helpful comments on a previous version of the manuscript. The work of M. d. C. is supported by Ministero dell'Università e Ricerca (MUR) (Bando PRIN 2017, Codice Progetto: 20179ZF5K5_006) and by INFN (Iniziative specifiche QUAGRAP and GeoSymQFT). The work of R. O. is supported by the Région Île-de-France within the DIM ACAV$^+$ project SYMONGRAV (Symétries asymptotiques et ondes gravitationnelles).

[1] S. A. Hayward, General laws of black hole dynamics, Phys. Rev. D **49**, 6467 (1994).
[2] Abhay Ashtekar and Badri Krishnan, Dynamical Horizons: Energy, Angular Momentum, Fluxes and Balance Laws, Phys. Rev. Lett. **89**, 261101 (2002).
[3] Ivan Booth and Stephen Fairhurst, The First Law for Slowly Evolving Horizons, Phys. Rev. Lett. **92**, 011102 (2004).
[4] Abhay Ashtekar and Badri Krishnan, Isolated and dynamical horizons and their applications, Living Rev. Relativity **7**, 10 (2004).
[5] Ivan Booth, Black hole boundaries, Can. J. Phys. **83**, 1073 (2005).
[6] Eric Gourgoulhon and Jose Luis Jaramillo, New theoretical approaches to black holes, New Astron. Rev. **51**, 791 (2008).
[7] E. Babichev, V. Dokuchaev, and Yu. Eroshenko, Backreaction of accreting matter onto a black hole in the Eddington-Finkelstein coordinates, Classical Quantum Gravity **29**, 115002 (2012).
[8] Masashi Kimura, Tomohiro Harada, Atsushi Naruko, and Kenji Toma, Backreaction of mass and angular momentum accretion on black holes: General formulation of metric perturbations and application to the Blandford–Znajek process, Prog. Theor. Exp. Phys. **2021**, 093E03 (2021).
[9] Kouji Nakamura, Proposal of a gauge-invariant treatment of $l = 0$, 1-mode perturbations on Schwarzschild background spacetime, Classical Quantum Gravity **38**, 145010 (2021).
[10] J. A. H. Futterman, F. A. Handler, and R. A. Matzner, *Scattering from Black Holes*, Cambridge Monographs on Mathematical Physics (Cambridge University Press, Cambridge, England, 2012).
[11] A. A. Starobinsky, Amplification of waves reflected from a rotating "black hole", Sov. Phys. JETP **37**, 28 (1973).
[12] F. S. Guzman and F. D. Lora-Clavijo, Spherical nonlinear absorption of cosmological scalar fields onto a black hole, Phys. Rev. D **85**, 024036 (2012).
[13] Valerio Faraoni, Andrea Giusti, and Bardia H. Fahim, Vaidya geometries and scalar fields with null gradients, Eur. Phys. J. C **81**, 232 (2021).
[14] Richard Brito, Vitor Cardoso, and Paolo Pani, Superradiance: New frontiers in black hole physics, Lect. Notes Phys. **906**, 1 (2015).
[15] Rodrigo Vicente and Vitor Cardoso, Dynamical friction of black holes in ultralight dark matter, Phys. Rev. D **105**, 083008 (2022).
[16] Harry Bateman and Arthur Erdélyi, *Higher Transcendental Functions*, California Institute of Technology. Bateman Manuscript Project Vol. 1 (McGraw-Hill, New York, NY, 1955).
[17] Marco de Cesare and Roberto Oliveri, Evolving black hole with scalar field accretion, Phys. Rev. D **106**, 044033 (2022).
[18] Ivan Booth, Lionel Brits, Jose A. Gonzalez, and Chris Van Den Broeck, Marginally trapped tubes and dynamical horizons, Classical Quantum Gravity **23**, 413 (2006).
[19] S. A. Hayward, R. Di Criscienzo, L. Vanzo, M. Nadalini, and S. Zerbini, Local Hawking temperature for dynamical black holes, Classical Quantum Gravity **26**, 062001 (2009).
[20] Lam Hui, Wave dark matter, Annu. Rev. Astron. Astrophys. **59**, 247 (2021).
[21] Carlos A. R. Herdeiro and Eugen Radu, Kerr Black Holes with Scalar Hair, Phys. Rev. Lett. **112**, 221101 (2014).

[22] Dina Traykova, Rodrigo Vicente, Katy Clough, Thomas Helfer, Emanuele Berti, Pedro G. Ferreira, and Lam Hui, Relativistic drag forces on black holes from scalar dark matter clouds of all sizes, arXiv:2305.10492.

[23] Alejandro Cruz-Osorio, Luciano Rezzolla, Fabio Duvan Lora-Clavijo, José Antonio Font, Carlos Herdeiro, and Eugen Radu, Bondi-Hoyle-Lyttleton accretion onto a rotating black hole with ultralight scalar hair, arXiv:2301.06564.

[24] Caio F. B. Macedo, Luíz C. S. Leite, Ednilton S. Oliveira, Sam R. Dolan, and Luís C. B. Crispino, Absorption of planar massless scalar waves by Kerr black holes, Phys. Rev. D **88**, 064033 (2013).

[25] Luiz C. S. Leite, Luís C. B. Crispino, Ednilton S. de Oliveira, Caio F. B. Macedo, and Sam R. Dolan, Absorption of massless scalar field by rotating black holes, Int. J. Mod. Phys. D **25**, 1641024 (2016).